scientific reports

Check for updates

OPEN

Accelerated mass loss of glaciers across Alaska since the Little Ice Age

Jonathan L. Carrivick[1]✉, Robert McNabb[2], Bethan J. Davies[3], Laura J. Larocca[4], Elizabeth Stephens[1], Rebecca Barry[1], Jenna L. Sutherland[5], Johannes Reinthaler[6,7], Jack Mason[2] & Ethan Lee[8]

Alaskan glaciers presently dominate contributions to global glacier mass loss and are projected to do so throughout the 21st Century. Here we assess centennial-scale evolution and mass loss of 5289 Little Ice Age (LIA) glaciers by mapping geomorphological evidence of glacier extent and by reconstructing ablation area ice surfaces. We find that Alaskan glaciers have experienced extensive fragmentation and have lost at least 19 ± 2.8% total area since the local LIA maximum (year 1810) to year 2008. Individual glaciers had a median area loss of 32 ± 4.7%. Our ice surface reconstruction for LIA glacier ablation areas leads to a total volume loss estimate of at least 3345 ± 836 km^3, equating to a mass loss of at least 2844 ± 711 Gt and a sea level equivalent of 8 ± 2 mm. Glacier mass balance since the LIA to 2008 was − 0.09 ± 0.02 m w.e. yr^{-1}, which, compared with − 0.67 ± 0.13 m w.e. yr^{-1} between 2000 and 2019, suggests a 7.4 ± 2.0 times acceleration across Alaska. Three quarters of Alaskan mountain regions shifted from near equilibrium mass balance between the LIA and 2008 (c. − 0.01 m w.e. yr^{-1}) to substantial mass loss (more negative than − 0.7 m w.e. yr^{-1}) between 2000 and 2019. Our Glacier Bay LIA icefield reconstruction evidences the greatest fragmentation, area, volume and mass loss of any known single LIA glacier globally. Our mapping, glacier reconstructions and mass loss findings will serve glacier evolution modelling, inform proglacial systems analysis, and support ecosystem services management especially within protected areas.

Mountain glaciers in Alaska were the greatest contributors to global mean sea level rise compared with any world region between 1976 and 2005[1]. Rates of Alaskan glacier mass loss have accelerated since the mid 1970s[2] and were − 83.1 ± 7.6 Gt yr^{-1} between 2010 and 2020[3], and − 66.7 ± 10.9 Gt yr^{-1} between 2000 and 2019[4]. Given these accelerated rates of mass loss from Alaskan glaciers[2,5,6,7], projections suggest that Alaska will likely retain its status as the largest regional contributor to global mean sea-level rise by 2100 regardless of the future emissions scenario[8]. However, whether Alaska has been such a dominant contributor of glacier mass loss over a longer (centennial) time scale is unknown.

A longer-term context of glacier evolution is needed to provide a baseline dataset from which subsequent changes can be compared, to spin up numerical models, and to provide insights into controls on centennial-scale glacier changes. As recently highlighted[9], glacier evolution models are largely calibrated using remote sensing-derived observations since the early 2000s or longer-term in situ observations that are available for only a small subset of glaciers worldwide[10]. However, at present these data are insufficient to robustly constrain model parameters and nonlinear feedbacks, including glacier mass balance responses to glacier fragmentation and separation of tributaries that induce major hypsometric shifts[7], and terminus environment changes (e.g. from marine to land, and from land to lake). Historical photographs and expedition records can also extend glacier reconstructions back in time[7,9,11,12], but again only for a limited number of glaciers and only up to a century ago.

Considering this paucity of empirical data, the former extent of Alaskan glaciers can usefully be reconstructed by exploiting the geomorphological imprint left during glacier advance during the Little Ice Age (LIA)[12], which across most of world regions occurred three to four centuries ago. Recent inventory-style reconstructions have

[1]School of Geography and water@leeds, University of Leeds, Leeds LS2 9JT, UK. [2]School of Geography and Environmental Sciences, Ulster University, Cromore Rd, Coleraine BT52 1SA, UK. [3]School of Geography, Politics and Sociology, Newcastle University, Newcastle upon Tyne NE1 7RU, UK. [4]School of Ocean Futures, Arizona State University, Tempe, AZ, USA. [5]School of Built Environment, Engineering and Computing, Leeds Beckett University, Leeds LS1 3HE, UK. [6]Department of Geography, University of Zurich, Zurich, CH, Switzerland. [7]Hazard Prevention Division, Federal Office for the Environment, Bern, CH, Switzerland. [8]School of Geography and Planning, University of Sheffield, Sheffield S3 7ND, UK. ✉email: j.l.carrivick@leeds.ac.uk

enabled quantification of glacier area, volume and mass changes across Greenland[13,14], New Zealand's Southern Alps[15], the Himalaya[16] and the Andes[17]. However, despite the importance of Alaska's contribution to global glacier mass loss in recent decades, there is a lack of knowledge regarding glacier evolution and contribution to sea level rise on a centennial-scale. The aim of this study is to quantify glacier area and volume changes across Alaska since the LIA. We achieve this aim using a geomorphological-based inventory-style mapping and ice surface reconstruction approach.

Datasets and methods

There are ~27,100 glaciers in Alaska (Randolph Glacier Inventory[18], RGI v6.0). The RGI was mapped using satellite images from years 2000 to 2011 with a mean year of 2008. Our mapping of Alaskan glaciers during the LIA covers 52 mountain regions (Fig. 1, Fig. SI_1) as defined within the Global Mountain Biodiversity Assessment (GMBA[19] Mountain Inventory v2. These mountain regions and glaciers span a climatic gradient, from very high precipitation and relatively warm 'maritime' conditions on the Pacific Coast to relatively dry cold 'high Arctic' conditions across the Brooks Range (Fig. 1). This climatic gradient dictates spatial patterns of glaciological conditions, soil development and vegetation.

Whilst the RGI now has a version 7.0, we started our mapping before its release, and there is little difference between the versions for Alaskan glaciers. In RGI v6.0, Alaskan glaciers collectively cover ~86,700 km². In this study, for practicality of mapping, we focussed on the 5675 glaciers > 1 km², which comprise just 21% of the total number but represent 93% (80,300 km²) of the total glacier area in Alaska. Of these Alaskan glaciers > 1 km², 97% are land-terminating, 0.9% are marine-terminating, and 2% are lake-terminating, as classified bythe RGI v6.0.

Our mapping protocol is fully described in the Supplementary Information (SI) and is based on definition of moraine ridge crests and trimlines visible in high resolution (< 5 m) satellite and aerial imagery, as well as hillshaded Digital Elevation Models (DEMs); primarily the 2 m resolution ArcticDEM[20]. We first identified and mapped moraine ridges dated to the LIA in the literature (Fig. SI_2). We then mapped contiguous geomorphology in neighbouring valleys. Repeat mapping of a subset of glaciers by different individuals revealed up to 15% difference in median glacier area change (Tables SI_1 and SI_2). A sensitivity test of the effect of only mapping RGI glaciers larger than 1 km² showed that if LIA outlines were mapped for all RGI glaciers, then the total LIA area could be up to 15% greater (Table SI_3). Relative area changes are calculated as a percentage of the LIA area. Uncertainty in our mapping of LIA glacier outlines is largely due to interpretation of geomorphology and is estimated to be ± 15% for groups (mountain regions, drainage basins, types) of glaciers (SI Sect. 2.3).

Our mapped LIA glacier outlines were analysed to determine LIA ablation areas, which were defined with an estimate of the Equilibrium Line Altitude (ELA) using the Area-Altitude Balance Ratio (AABR) method[21]. Full details of our workflow, which is the prevailing approach used for inventory-style LIA glacier reconstructions[13,14,15,16,17] are in our SI (Sect. 2.1); briefly we reconstructed LIA ice surfaces for the LIA ablation areas using a natural neighbour interpolation between point elevations extracted along the ablation area perimeter (i.e. from the ELA across each glacier and from points along the moraine crests). Elevations were extracted from the ALOS World 3D 30 m DEM (AW3D30)[22,23]. The difference between this reconstructed LIA ice surface and the present topography as provided by the DEM produced surface lowering or ice thickness change and hence volume change. The DEM has 30 m resolution, is largely artefact-free and void-free across Alaskan glaciers, but most importantly has a median date of 2008 (range from 2006 to 2011), which corresponds to the mean date of the RGI v6.0 glacier outlines. Whilst we were able to estimate the submarine volume of LIA ice (SI Sect. 2.2), our volume change estimates remain conservative as we assume no volume change in glacier accumulation areas, and more importantly we cannot account for sediment or lake water infilling the valleys (see the SI for more detail). Our LIA ice surface and volume change estimates have uncertainty of ± 25% for groups of glaciers (SI Sect. 2.4).

We use the year 1810 as a median date for the timing of the most recent and extensive glacier advance during the LIA (coinciding with the Dalton Minimum, ~1790 to 1830; SI Sect. 2.5). We consider the period from 1750 to 1880 to define upper and lower bounds when calculating area and change rates. Our calculations of acceleration (i) assume that the rate of change of glaciers between the LIA and the RGI/DEM date (2008) has been constant, and (ii) are reported as conservative estimates as there is overlap between the two time periods of comparison (i.e. LIA to 2008 and 2000 to 2019; Table SI_4).

Results

Alaskan glaciers covered 100,729 ± 15,109 km² during the LIA, which indicates a loss of at least 19,160 ± 2874 km² or 19 ± 2.8% since the LIA (year 1810) to 2008, i.e. a mean rate of -0.1 ± 0.01% yr^{-1}. Of the 52 individual regions (Fig. 1) named in Figure SI_1, the Fairweather Range in south-east Alaska has had the largest absolute glacier area loss of at least 2827 ± 424 km² or 44 ± 6.6% (Table SI_6). The Southern Icefield Ranges, Chugach Mountains east, Chugach Mountains west and Takhinsha Mountains have all lost > 1000 km² glacier area since the LIA. The aforementioned Fairweather Range, Brooks Range, Takhinsha Mountains and the Spectrum Range regions have all lost > 40 ± 6% LIA area (Fig. 1; Fig. SI_3; Table SI_6). As these regions have relatively small glaciers (Table SI_6), the high area loss is expected since relative area changes are usually higher for smaller glaciers[24].

The 5289 LIA glaciers mapped in this study comprise 9881 RGI v6.0 glaciers. Many LIA glaciers were composed of tens of RGI glaciers, indicating extensive fragmentation. In the exceptional case of the Glacier Bay LIA icefield, that LIA glacier was composed of > 100 coalesced RGI glaciers. This fragmentation has occurred by disintegration of former tributaries or, in some cases, by separation of upper parts from ablation tongues (Fig. 2A).

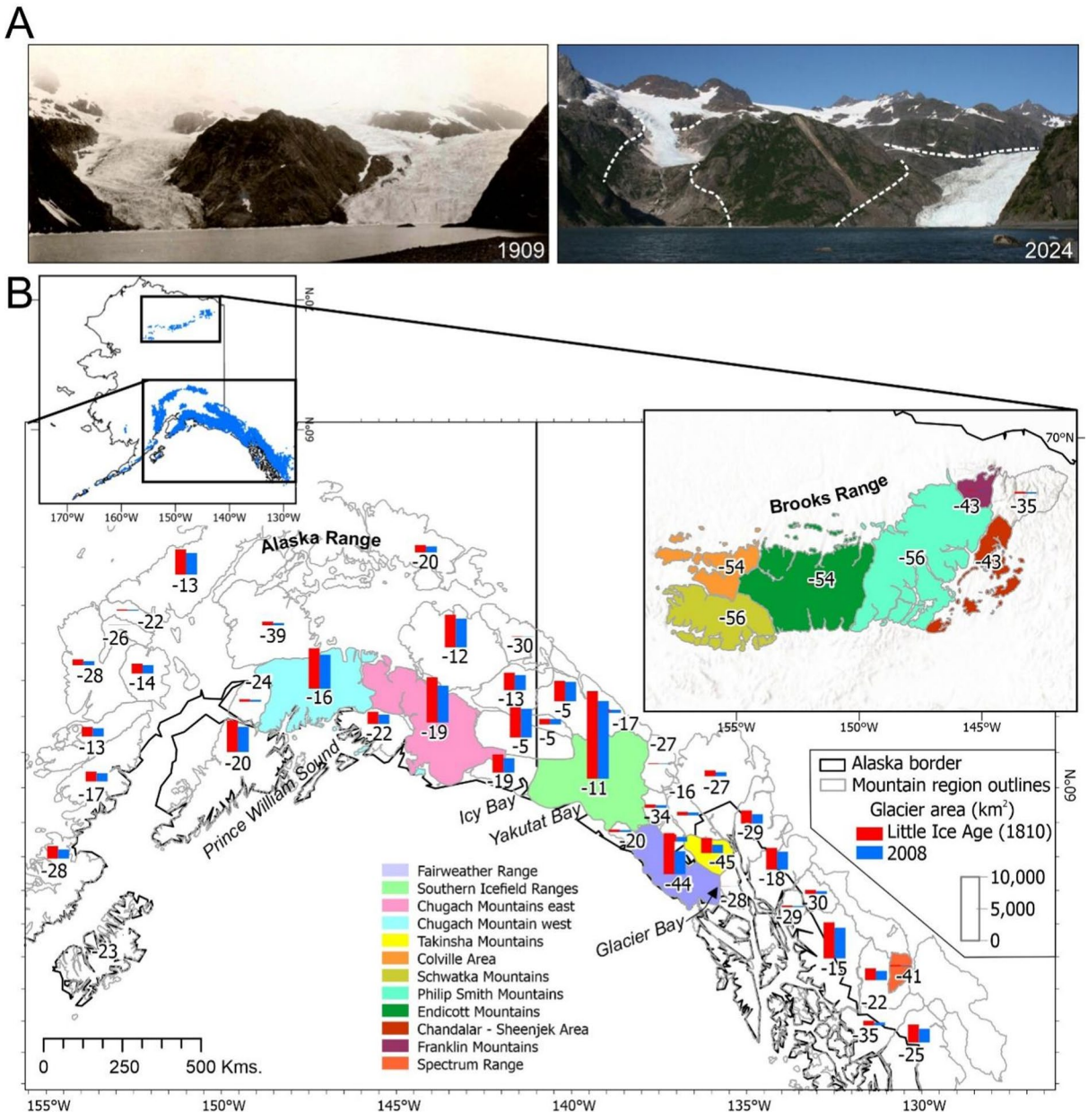


Fig. 1. Glacier change evidenced by repeat oblique photography in Panel A of Holgate Glacier in Aialik Bay, Kenai Fjords National Park; 1909 image by Higgins (1909) and 2024 image by Cooper (2024). White dashed lines on 2024 image are moraine ridge crests and trimlines interpreted to mark the glacier extent during the LIA. Panel B is a comparison per mountain region of our mapped Little Ice Age (year 1810) glacier area total, and the total glacier area in 2008. Labels on bar charts report percentage glacier area change; the percentage difference between each pair of red and blue columns. The inset Alaska outline map shows RGI glaciers (blue). Note that Brooks Range has the same bar scale for comparison. Only mountain regions mentioned in the text are coloured and listed for clarity in this figure, but all are labelled for reference in Figure SI_1.

On an individual glacier basis, the median absolute area change between the LIA and year 2008 was just -0.95 ± 0.14 km^2 for the whole time period with an inter-quartile range of -2.04 ± 0.31 km^2 to -0.44 ± 0.07 km^2. The median relative glacier area change was $-32 \pm 4.8\%$ ($0.16 \pm 0.02\%$ yr^{-1}) with an inter-quartile range from $-45 \pm 6.8\%$ to $-21 \pm 3.2\%$. Overall, larger glaciers lost the most area in absolute terms ($r^2 = 0.59$, $p < 0.01$; Fig. SI_4A), whilst smaller glaciers lost the most area relative to the LIA extent ($r^2 = 0.18$, $p < 0.01$; Fig. SI_4B).

Ice thickness change (surface lowering within LIA ablation areas, from the LIA to year 2008), was median 35 ± 9 m. The standard deviation of ice thickness change was 25 ± 5 m. Five glaciers had mean ice thickness change of $> 200 \pm 50$ m (Fig. 2B) e.g. Melbern Glacier (Fairweather Range), Guyot Glacier (Robinson Mountains), or Columbia Glacier (Chugach Mountains west). At the highest end, Columbia Glacier had maximum ice thickness change of up to 500 ± 125 m, and the Glacier Bay LIA icefield $> 1000 \pm 200$ m.

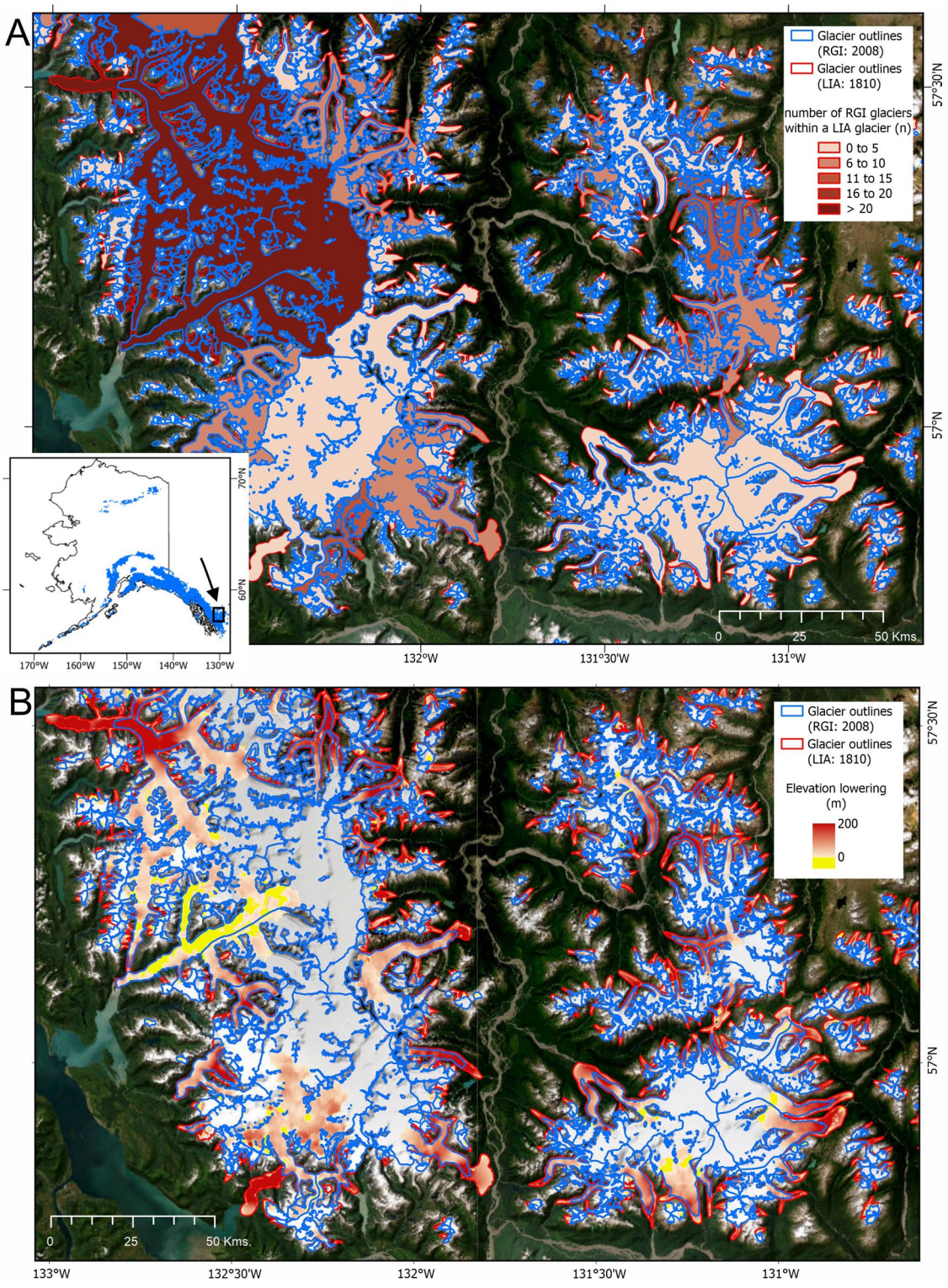


Fig. 2. Example of our mapping for the southern part of the Central Boundary Ranges and for the Stikine-Ambition Area. Panel A shows the number of extant glaciers (year 2008) within each LIA (year 1810) glacier outline, evidencing massive fragmentation. Panel B depicts surface lowering calculated between our reconstructed LIA glacier ablation area surface and 2008.

The total volume loss of Alaskan glaciers since the LIA has been at least 3345 ± 836 km^3 (Table SI_7). We find a correlation of $r^2 = 0.8$ ($p < 0.01$) between area loss and volume loss (Fig. SI_5), indicating that glaciers experiencing greater areal retreat also tended to experience greater volume loss. The median volume loss of individual glaciers is 0.04 ± 0.01 km^3, but variability is high (standard deviation = 14.8 km^3), indicating that a

small number of glaciers experienced disproportionately large losses. The greatest volume loss (1008 ± 252 km^3) occurred at the Glacier Bay LIA icefield, which spanned the Fairweather Range and Takhinsha Mountains. The other highest volume losses for individual LIA glaciers occurred at Columbia Glacier (Chugach Mountains west, 114 ± 29 km^3), Hubbard Glacier (Southern Icefield Ranges, 136 ± 34 km^3), and 'Icy Bay Glacier' (Robinson Mountains, 96 ± 24 km^3). The total volume loss of glaciers across Alaska since the LIA suggests a mass loss of at least 2844 ± 711 Gt, assuming an ice density of 850 kg m^3, and produces a sea level equivalent of at least 8 ± 2 mm (see SI for methods).

Across Alaska, the mean centennial mass balance from year 1810 to 2008 was − 0.09 ± 0.02 m w.e. yr^{-1}. When compared with the − 0.67 ± 0.13 m w.e. yr^{-1} for 2000 to 2019 that Hugonnet et al.[4] report for Alaska, we evidence a 0.58 ± 0.15 m w.e. yr^{-1} difference and thus an overall 7.4 ± 2.0 times acceleration in the rate of glacier-specific mass loss. Individual regions have even higher mass loss acceleration factors but these tend to be regions that had near equilibrium rates (< 0.1 m w.e. yr^{-1}) between LIA and 2008, e.g. Auriol Range: 7.7 ± 1.9 times, Brabazon Range: 16.4 ± 4.1 times, Chigmit Mountains: 12.2 ± 3.1 times, Chilkat Range: 5.1 ± 1.3 times, Chugach Mountains east: 11.2 ± 2.8 times, Endicott Mountains: 13.7 ± 3.4 times, Granite Range: 10.3 ± 2.5 times, Neacola Mountains: 9.3 ± 2.3 times, Schwatka Mountains 7.8 ± 1.9 times, Talkeetna Mountains: 9.2 ± 2.3 times and Tordrillo Mountains: 10.4 ± 2.6 times (Fig. 3). The median change in glacier mass balance was − 0.56 ± 0.14 m w.e. yr^{-1}, corresponding to a 7.7 ± 1.9-fold acceleration in mass loss. Mass balance has also become more variable since the LIA. For the 2000 to 2019 period, the median mass balance of mountain regions in this study was − 0.67 ± 0.13 m w.e. yr^{-1}, the most negative mass balance of any mountain region was − 1.5 ± 0.35 m w.e. yr^{-1} and the inter-quartile range was 0.35. In contrast, during the LIA to 2008 period, the median mountain region mass balance was almost an order of magnitude less at -0.09 ± 0.01 m w.e. yr^{-1}, the most negative mass balance of any region was − 0.54 ± 0.14 m w.e. yr^{-1} and the inter-quartile range was just 0.06 (Table SI_7).

We also find that glacier change since the LIA differed among glacier terminus types. Assuming that that rates of change remained constant between the LIA and year 2008 (and taking the mean rate between year 2000 and 2019[4]), the distributions of absolute area change (Fig. 4A), relative area change (Fig. 4B), and volume and

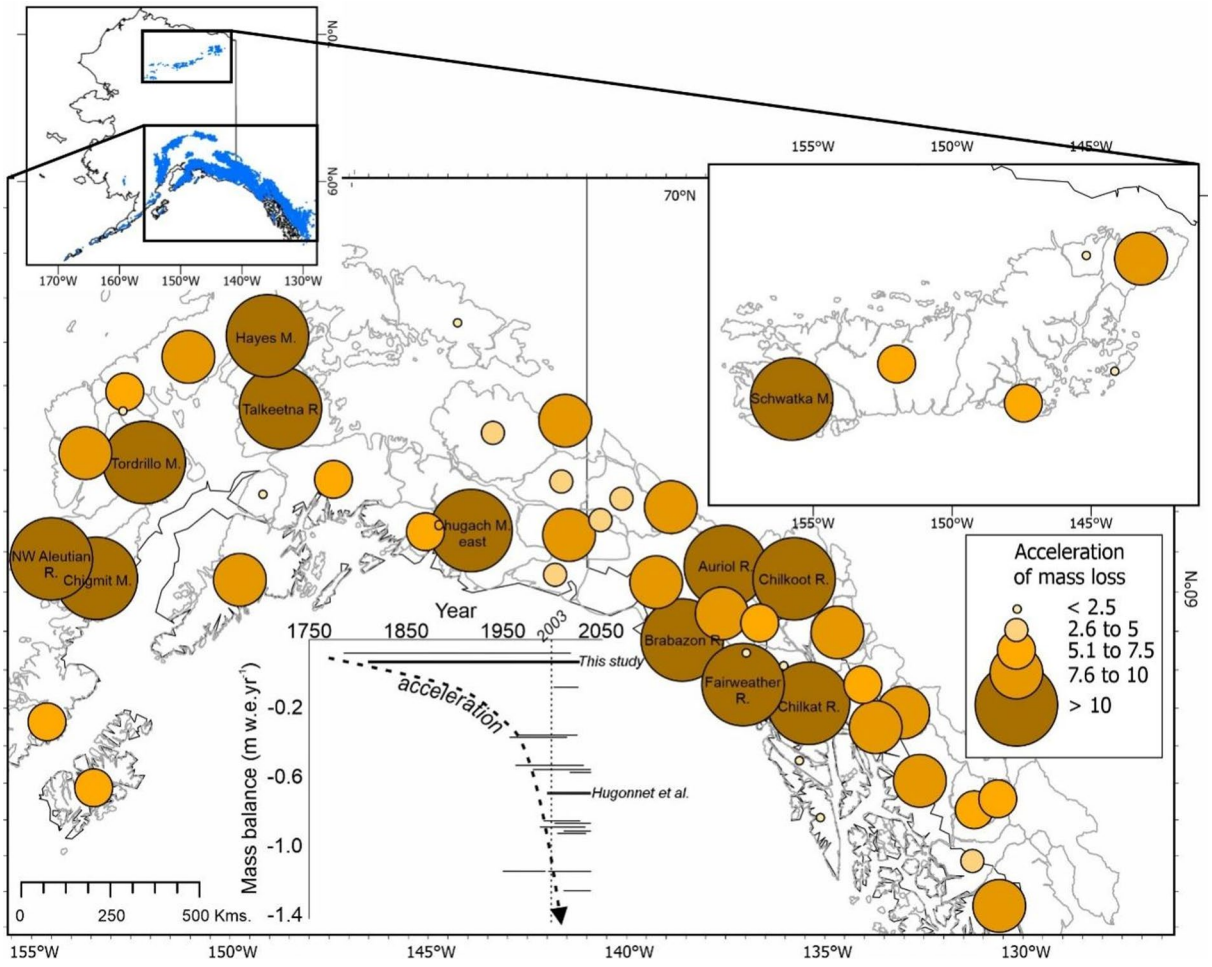


Fig. 3. Acceleration in specific mass loss per mountain region, calculated as a multiplier between the mean glacier mass balance from LIA (year 1810) to 2008 and the mean glacier mass balance from 2000 to 2019. Inset graph shows mass balance rates since the LIA compared to rates reported in the literature (Table SI_8) during the 20th and 21st Centuries.

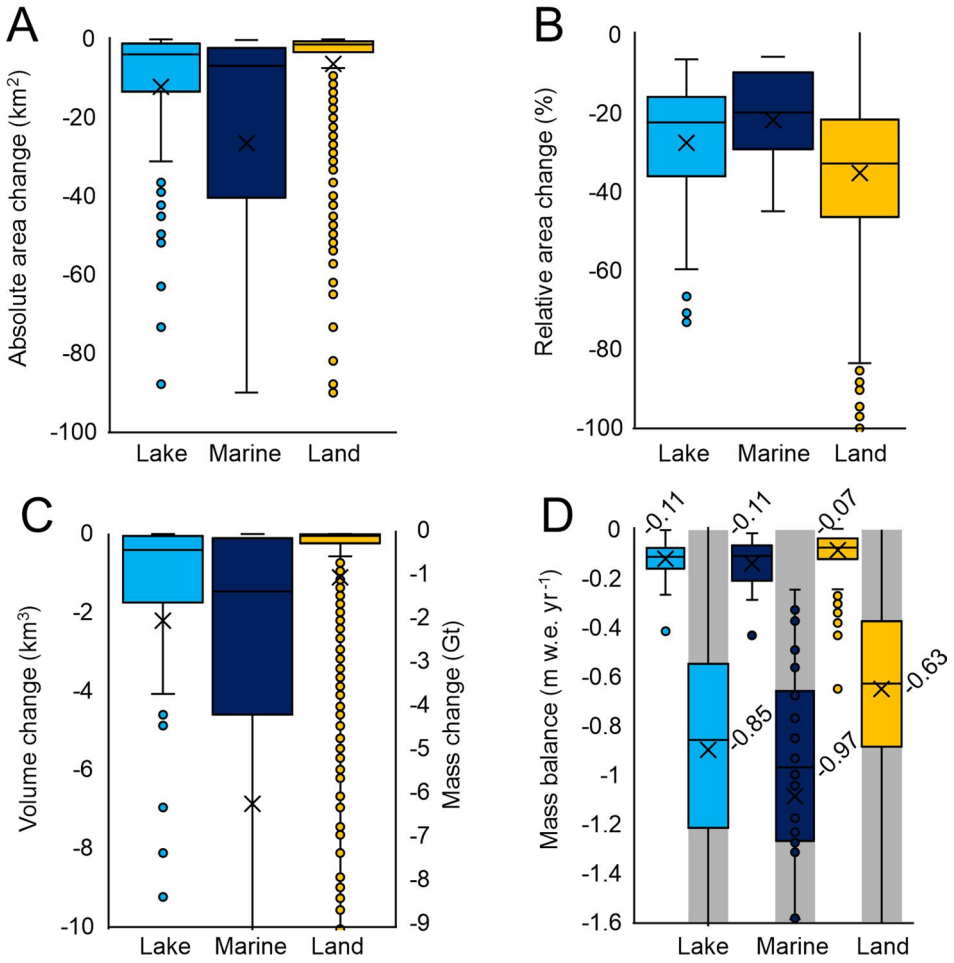


Fig. 4. Glacier changes across Alaska categorised by glacier terminus type. The panels show centennial-scale changes in absolute (**A**) and relative (**B**) area, volume (**C**) and mass (**D**) all since the LIA (year 1810), and mean mass balance during 2000 to 2019 [4], denoted by grey-shade background (**D**). Boxes are the interquartile range, horizontal bars are the median, X is the mean, the vertical line extends between the minimum and maximum, excluding outliers, and coloured dots are outliers. Note a few outliers are omitted by clipping the y axes for clarity of depicting the majority of the dataset in the boxes. Labels in (D) are medians.

mass change (Fig. 4C-D) show that mean glacier mass loss rates during 2000 to 2019 were 6.8 ± 1.7, 7.7 ± 1.9, and 8.2 ± 2.0-fold greater than the long-term centennial rate (LIA (1810) to 2008) for lake-, land-, and marine-terminating glaciers, respectively (Fig. 4D). However, we cannot attribute the differences in retreat rates entirely to terminus-type because marine-terminating glaciers in Alaska tend to be much larger than other types and have a differing hypsometry. Furthermore, Fig. 4D indicates that whilst centennial-scale mean mass balances were broadly similar among glacier types, mass balance between 2000 and 2019 had more variability both between and within glacier type groups.

Discussion

The lack of a spatial pattern in centennial-scale glacier area losses (Fig. 1) and the strong spatial heterogeneity in centennial-scale mass loss acceleration (Fig. 3) are difficult to interpret. The former hints towards a forcing that is Alaska-wide, whilst the latter suggests that local factors such as topography and glaciology are important, as will be discussed below. An Alaska-wide forcing could be global climate change. Specifically, the LIA across Alaska was recently suggested to have been characterised by a weaker westward-shifted Aleutian low (a synoptic weather system) and overall colder and drier conditions relative to present[25].

How fast are modern rates of glacier mass loss across Alaska?

The acceleration in mass loss that we report across Alaska is supported by reports of rising snowlines[26] and Equilibrium Line Altitude (ELA)[25,27], and geodetic (DEM-derived) losses[9], for example, but our datasets and findings add considerable spatial coverage and spatio-temporal detail. This is the first study of LIA glacier changes across Alaska. It is also the first study to include inventory-style glacier-specific analysis of number, area, surface, lowering, volume, mass changes.

The inset panel of Fig. 3 and Table SI_8 compare the Alaska-wide centennial-scale mass loss rates computed in this study to mass loss rates that we have derived from the literature over a range of spatial and temporal scales. This comparison shows that less negative estimates of mass loss -0.48 ± 0.1 m w.e. yr^{-1} and -0.49 ± 0.1 m w.e. yr^{-1} pertain to the earlier time periods of 1962 to 2006[5], and the mid-1950s to the mid-1990s[28], respectively. Contrastingly, the faster rates of mass loss of -0.96 ± 0.1 m w.e. yr^{-1} and -0.97 ± 0.1 m w.e. yr^{-1} pertain to more recent time periods of 2010 to 2020[3] and 2003 to 2007[29], respectively. The rate of -0.67 ± 0.13 m w.e. yr^{-1} computed for 2000 to 2019[4], -0.85 m w.e. yr^{-1} for 2006 to 2016[30] and -1.26 ± 0.61 m w.e. yr^{-1} for 2015 to 2024[2] all fit the temporal pattern of acceleration. Other comparisons, such as for Juneau icefield[6] are included in the inset to Fig. 3 and Table SI_8.

By any estimate the reconstructed Glacier Bay LIA icefield in the Fairweather Range (Fig. 1) is truly exceptional. We are not aware of any other glacier in the world that has lost so much area, fragmented so much, and lost so much volume so fast. For context our computed volume loss of at least 1008 ± 252 km^3 for the Glacier Bay LIA icefield is ~ 1.7 times greater than the 587 km^3 volume loss reported for all glaciers and ice caps across Greenland since the LIA[14], and more than double the 390 to 586 km^3 volume loss reported for the Himalaya since the LIA[16]. It is approximately 3.5 times the 283 km^3 volume (not volume loss) modelled for the European Alps glaciers during the LIA[31]. Our estimate of volume loss of the Glacier Bay LIA icefield does not agree with the 2500 km^3 and 3030 km^3 estimates by Larsen et al.[32,33]. The independent evidence that we used to reconstruct the Glacier Bay icefield and our reconstruction method are detailed in our SI. Unfortunately, whilst their 2005 study mentioned geomorphological evidence and thinning of up to 1500 m, their method of LIA ice surface reconstruction and hence their volume change calculation is unclear. This may be because the emphasis of their work was on explaining isostatic uplift rates, rather than glacier mass change.

We therefore conducted some tests of our own ice surface reconstruction by comparison with an independent method whereby the pattern of recent elevation change rates for each glacier from Hugonnet et al.[4] is used to calculate glacier-specific elevation change gradients across an entire glacier[34,35]. These tests show that our ablation-area only method produces volume change estimates that are low compared to the elevation-change gradient method (Fig. SI_6A). That supports our assertion that our volume change calculations are conservative, not least because we restrict our analyses to LIA ablation areas. The elevation-change gradient estimates could also be too high due to an implicit assumption that thinning of glaciers has been occurring since the LIA within accumulation areas. That assumption is debatable given widespread recognition that glacier mass loss[3,7,9], glacier equilibrium line altitude[36] and end of summer snowline elevation rises[37] have accelerated mostly in recent decades. Furthermore, we find that in some other Alaskan mountain regions within our study area there is no agreement between the two volume change estimates (Fig. SI_6B), which suggests that the pattern of thinning in recent decades is not representative of the long-term centennial pattern e.g. [13,17], perhaps due to the formation and expansion of terminus lakes e.g. [14,15,16] and debris cover[15], surge type glaciers, and the impact of glacier size and hypsometry[7] on glacier response time.

In the case of the Glacier Bay LIA icefield, the elevation-change gradient method produces a volume loss of 1041 km^3 (compared to our 1008 km^3), with a portion above sea level of 830 km^3. However, the ice surface estimated by the elevation-change gradient method is unrealistic with artefacts especially at the boundary between proglacial land and contemporary ice where LIA glaciers were marine-terminating (Fig. SI_6C). Similar patterns are observed for lake-terminating glaciers, and for glaciers that have recently advanced, including having surged. Given the uncertainties and unrealistic patterns in the elevation-change gradient method outputs, we conclude that the differences with our estimates do not reflect negatively on this study, and we have confidence in our Glacier Bay icefield reconstruction.

The massive area and volume loss of the Glacier Bay LIA icefield that we evidence compared to other Alaskan glaciers is most simply explained by tidewater glacier dynamics. Specifically, a 'tipping point' can occur for tidewater glaciers when they change from being grounded to floating and thereon become strongly affected by additional thermo-mechanical forcings, notably tidal flexure and fracture and incursion of warm ocean currents beneath the glacier[38,39,40], as well as by fjord geometry[41,42]. Accordingly, Alaskan glaciers that terminate in the ocean today, such as Guyot, Yahtse, and Tyndall glaciers in Ice Bay (Robinson Mountains), and Hubbard Glacier (Southern Icefield Ranges), LeConte Glacier (central Boundary Ranges), and Columbia Glacier (Chugach Mountains west), have had exceptional volume change during recent decades[43]. The latter has been one of the world's most rapidly changing glaciers with 0.5 km yr^{-1} retreat between 1985 and 2013[43,44].

Comparison of our conservative estimates of glacier mass loss from the LIA (1810) to 2008 with rates computed for 2000 to 2019 reveals a clear acceleration in glacier mass loss across Alaska. This finding is supported by the large number of glaciers analysed, the Alaska-wide spatial coverage, and the high density of studied glaciers within individual mountain ranges (often hundreds per mountain region). We suggest that this acceleration reflects substantially higher mass loss rates since the latter half of the 20th Century, as well as the emergence of stronger regional contrasts in glacier change (i.e., rates of mass loss were considerably more uniform across Alaska between the LIA and 2008 than during the post-2000 period; Fig. 4D, Table SI_7). Across Alaska, the present-day rate of glacier mass loss greatly exceeds the centennial-scale mean rate by more than a factor of 5 in many regions, and by up to a factor of 15 (Fig. 3; Table SI_7). These acceleration estimates are conservative. If only the last 15 years of the Hugonnet et al.[4] dataset are considered (i.e. 2005 to 2019), thereby minimizing the overlap with our LIA to 2008 reconstruction period, the estimated acceleration increases from 5.8-fold to 6.3-fold for glacier mass loss (Gt yr^{-1}), and from 5.9-fold to 6.4-fold for glacier mass balance (m w.e. yr^{-1}) (Table SI_3).

The similarity in mean mass balance change among glacier terminus types on a centennial timescale, together with the low variability within each terminus type group (small interquartile range), suggests that glaciers were near steady state during the LIA and remained near equilibrium towards the early 20th Century. Accepting that the exact position of the 'curve of acceleration' in Fig. 3 is uncertain, it can be suggested that differences on a

centennial scale in glacier response associated with morphometric variables/setting become muted as glaciers have over ~200 years to adjust to climate forcing. In contrast, the stronger divergence in mass loss rates among glacier types during 2000 to 2019 may reflect transient responses under rapidly changing climate conditions. Whilst recognising the relatively early onset of tidewater glacier retreat in Alaska, e.g. Glacier Bay, Icy Bay, we interpret the increased rates of mass loss and variability between and within glacier terminus type in the last two decades (Fig. 4D) as evidence for an increased glacier disequilibrium[45]. Possible explanations for the degree of imbalance among glacier types include differences in glacier size, hypsometry, terminus type (land, lake, marine) and surface type/cover (debris, clean), factors that have been identified as important controls on glacier change in similar studies of LIA to present glacier evolution in Greenland[13,14], New Zealand's Southern Alps[15], the Himalaya[16] and the Andes[17].

Are the rates of glacier retreat and mass loss across Alaska since the LIA unusual in a global context?

Considering area changes, which have a lower uncertainty (more confidence) than volume or mass changes, Table SI_9 reports rates of glacier area change since the LIA to the present that have been calculated from published quantities of glacier area and LIA timing. As most of the studies used the same workflow as herein, results are directly comparable. The $-19 \pm 2.8\%$ area loss calculated in this study for Alaska is comparable to $-19 \pm 2\%$ for Jostedalsbreen, southern Norway[46], $-22 \pm 3.3\%$ for NE Greenland[13], $-24 \pm 3.4\%$ for the Southern Alps of New Zealand[15], and $-25 \pm 4\%$ for the Andes[17]. Other world regions have had greater centennial-scale glacier area loss rates (Table SI_9), e.g. $-40 \pm 8\%$ reported for the Himalaya[16] and $-57 \pm 4\%$ for the European Alps[35].

Accounting for differing timings of the LIA glacier maximum between world regions, our rate of glacier area change for Alaska since the LIA of $-0.1 \pm 0.01\%\ yr^{-1}$ is comparable to the $0.11 \pm 0.01\%\ yr^{-1}$ reported for the Andes[17], $-0.12 \pm 0.01\%\ yr^{-1}$ for Svalbard[47], the $-0.1 \pm 0.01\%\ yr^{-1}$ for Jotunheimen, Norway[48], and the $-0.1 \pm 0.01\%\ yr^{-1}$ reported for parts of the Himalaya[16]. Western Italy, Switzerland, Austria, the Altai all seem to have had much higher (up to three times) centennial rates of relative glacier area loss than Alaska (Table SI_9), which could be due to the shorter time periods considered for these regions but also due to the fact that smaller glaciers tend to have shorter response times[49].

The acceleration in glacier mass loss across Alaska has been far greater than reported for Greenland, which had a 3 times acceleration compared with the time period 2000 and 2019[13,14]. Both the Southern Alps of New Zealand and Patagonia have experienced a doubling of mass loss comparing rates since the LIA to those in recent decades[17,50]. However, the region-wide acceleration in mass loss that we calculate for Alaska is not as fast as the ten-fold magnitude increase in Himalayan glacier mass loss in recent decades compared to the rates since the LIA[16]. We compute that one third of Alaskan mountain regions have mass loss accelerations $> 8 \pm 2$ times. The Alaskan regions that have experienced accelerations in glacier mass loss $> 10 \pm 2.5$ times (Table SI_7) tend to have small(er) land-terminating glaciers with relatively fast-response times and can be interpreted to be the most rapidly changing high mountain landscapes of any world region.

Wider implications

Our dataset of LIA glacier areas along with the modelled LIA ice surface, volume and mass changes provides context to set current rates of glacier changes into a historical perspective. The observed glacier mass losses can be directly transformed into landcover changes[51] and hence albedo changes affecting radiative forcing and Earth's energy balance[52], complementing knowledge about climate change impacts around the world.

Moreover, the datasets presented herein will inform numerical modelling of glacier evolution. Specifically, we can provide a spatially-resolved glacier extent to serve as a baseline from which spin ups of glacier geometry can be run, for training models of glacier evolution, including those focusing on equilibrium line altitude changes[25], glacier disequilibrium[45] and response time[49], and for those numerical model simulations that are driven by, calibrated or bias-corrected to geodetic (sequential DEM) changes[9]. Our regionally aggregated mass changes will also be instructive for understanding wider impacts of deglaciation since the LIA, for example on isostatic uplift[31].

The LIA glacier outline dataset defines proglacial systems of greater than 4000 km^2 per major drainage basin that have emerged and evolved since the LIA[53,54](Fig. SI_7), including new coastlines[55]. The proglacial area expansions within the Alsek and Taku drainage basins account for 5.3% and 5.6% of the total drainage basin areas, respectively (Fig. SI_7). These proglacial systems are transitioning from glacial to paraglacial and periglacial conditions[56,57], and the related process regime shifts manifest in voluminous meltwater, creating and enlarging proglacial lakes[58], driving landscape instability and sediment yield[59], thereby controlling water quality e.g. [60] and aquatic ecosystems[61,62,63]. Glacial outburst floods[64] and landslides[65,66,67] are common across Alaska. These proglacial systems are within and across numerous protected areas (Fig. SI_8) that are internationally and nationally recognised for world heritage[68] and important societal benefits.

Summary and conclusions

In summary, we have quantified the number, area, volume change, mass change, and rates of change of those for glaciers across Alaska since the LIA. We have identified a marked acceleration in glacier change between 2000 and 2019 when compared to the long-term rate from the LIA. Our principal findings are:

(i) Alaska has not always been the dominant global contributor to glacier mass loss. The Alaska-wide centennial-scale rate of mass loss since the LIA is modest compared to other glaciated regions.
(ii) Across Alaska, glacier mass loss accelerated by at least a factor of 7 on average in recent decades, which is exceptional but not unique in global terms. Three quarters of Alaskan mountain regions shifted from near

equilibrium mass balance between the LIA and 2008 (c. −0.01 m w.e. yr^{-1}) to substantial mass loss (more negative than −0.7 m w.e. yr^{-1}) between 2000 and 2019.

(iii) Alaskan glacier area change and recent mass loss acceleration differ significantly among land-, lake-, and marine-terminating glaciers, highlighting the important role of morphometric variables and terminus setting in modulating glacier response to climate change.

To conclude, whilst Alaska has not been the dominant global contributor to glacier mass loss since the LIA, its Glacier Bay LIA icefield represents one of the most extreme examples of glacier change worldwide. Since the LIA, the Glacier Bay LIA icefield has fragmented into over 100 glaciers, lost > 3500 ± 525 km^2 (55 ± 8.3%) of its area, experienced > 1000 ± 250 m of ice-surface lowering, and lost > 1008 ± 252 km^3 of ice volume. These changes are truly exceptional; we are unaware of any other glacier in the world that has changed so dramatically since the LIA. Tidewater glacier dynamics provide a probable explanation for the magnitude of change observed in the Glacier Bay LIA icefield. We hypothesize that a transition from a grounded to floating marine-terminating system enhanced mass loss due to thermal-mechanical forcings. This interpretation is supported by the large volume losses observed for other Alaskan glaciers that terminate in the ocean today.

More widely, the quantification of past glacier and proglacial evolution derived in this study over timescales meaningful for future glacier and proglacial projections, provide baseline data useful for evaluating risks associated with landscape evolution from a glacial to periglacial system (e.g. glacial lake outburst floods, landslides, water quality), visualizing landcover and hence albedo change in remote areas with few measurements, and is essential data to train numerical models of glacier evolution.

Data availability

LIA glacier outlines, LIA glacier ablation areas, and mountain regions are available as vector files in geopackage and shapefile format as supplementary data files. The related attribute tables include number, area, volume and mass calculations for each glacier. Also the LIA ice surface and surface lowering grids are available as supplementary data files in raster format (.tif). The LIA glacier outlines will also be submitted to GLIMS.Mountain regions are from GMBA Mountain Inventory (Snethlage et al., 2022), River drainage basins and rivers are from Hydrosheds [https://www.hydrosheds.org/](https:/www.hydrosheds.org) and [https://www.hydrosheds.org/products/hydrorivers](https:/www.hydrosheds.org/products/hydrorivers) respectively, and protected areas are from [https://www.protectedplanet.net/en/thematic-areas/wdpa? tab=WDPA](https:/www.protectedplanet.net/en/thematic-areas/wdpa? tab=WDPA).

Code availability

The workflow described herein uses standard spatial analysis tools available in Geographic Information Systems. Code used for topological checking of LIA outlines, calculating area change between LIA and RGI outlines, and aggregating results to mountain ranges is available at https://github.com/iamdonovan/alaska_lia_outlines. Code used for compiling bathymetric datasets and calculating submarine ice volume is available at https://github.com/iamdonovan/ak_glacier_bathymetry.

Received: 6 April 2026; Accepted: 2 September 2026
Published online: 18 September 2026

References

1. Zemp, M. et al. Global glacier mass change in 2025. *Nat. Reviews Earth Environ.* **7**, 213–215 (2026).
2. Dussaillant, I. et al. Annual mass change of the world's glaciers from 1976 to 2024 by temporal downscaling of satellite data with in situ observations. *Earth Syst. Sci. Data.* **17** (5), 1977–2006 (2025).
3. Jakob, L. & Gourmelen, N. Glacier mass loss between 2010 and 2020 dominated by atmospheric forcing. *Geophys. Res. Lett.* **50** (8), e2023GL102954 . (2023)
4. Hugonnet, R. et al. Accelerated global glacier mass loss in the early twenty-first century. *Nature* **592** (7856), 726–731 (2021).
5. Berthier, E., Schiefer, E., Clarke, G. K., Menounos, B. & Rémy, F. Contribution of Alaskan glaciers to sea-level rise derived from satellite imagery. *Nat. Geosci.* **3** (2), 92–95 (2010).
6. Yang, R., Hock, R., Kang, S., Shangguan, D. & Guo, W. Glacier mass and area changes on the Kenai Peninsula, Alaska, 1986–2016. *J. Glaciol.* **66** (258), 603–617 (2020).
7. Davies, B. et al. Accelerating glacier volume loss on Juneau Icefield driven by hypsometry and melt-accelerating feedbacks. *Nat. Commun.* **15** (1), 5099 (2024).
8. Rounce, D. R. et al. Global glacier change in the 21st century: Every increase in temperature matters. *Science* **379** (6627), 78–83 (2023).
9. Wells, A. et al. An 85-year record of glacier change and refined projections for Kennicott and Root Glaciers, Alaska. *Nat. Commun.* **16** (1), 7835 (2025).
10. Zemp, M., Hoelzle, M. & Haeberli, W. Six decades of glacier mass-balance observations: a review of the worldwide monitoring network. *Ann. Glaciol.* **50** (50), 101–111 (2009).
11. Geyman, E. C., van Pelt, J. J., Maloof, W., Aas, A. C., Kohler, H. F. & J Historical glacier change on Svalbard predicts doubling of mass loss by 2100. *Nature* **601**, 374–379 (2022).
12. Larocca, L. J. et al. Greenland-wide accelerated retreat of peripheral glaciers in the twenty-first century. *Nat. Clim. Change.* **13** (12), 1324–1328 (2023).
13. Carrivick, J. L. et al. Accelerated volume loss in glacier ablation zones of NE Greenland, Little Ice Age to present. *Geophys. Res. Lett.* **46** (3), 1476–1484 (2019).
14. Carrivick, J. L. et al. Mass loss of glaciers and ice caps across Greenland since the Little Ice Age. Geophys. Res. Lett. **50** (10) eGL103950 (2023).
15. Carrivick, J. L., James, W. H., Grimes, M., Sutherland, J. L. & Lorrey, A. M. Ice thickness and volume changes across the Southern Alps, New Zealand, from the Little Ice Age to present. *Sci. Rep.* **10** (1), 13392 (2020).
16. Lee, E. et al. Accelerated mass loss of Himalayan glaciers since the Little Ice Age. *Sci. Rep.* **11** (1), 24284 (2021).

17. Carrivick, J. L. et al. Accelerating glacier area loss across the Andes since the Little Ice Age. *Geophys. Res. Lett.* **51** (13), e2024GL109154 (2024).
18. GLIMS. Global land ice measurements from space: Glacier database. (2021). Retrieved from https://www.glims.org/glacierdata/ last accessed February 2026.
19. Snethlage, M. A. et al. A hierarchical inventory of the world's mountains for global comparative mountain science. *Nat. Sci. Data*. **9** (1), 149 (2022).
20. Porter, C. et al. ArcticDEM, Version 4.1. *Harv. Dataverse V1*. https://doi.org/10.7910/DVN/3VDC4W (2023). Last accessed Dec 2025.
21. Oien, R. P., Rea, B. R., Spagnolo, M., Barr, I. D. & Bingham, R. G. Testing the area–altitude balance ratio (AABR) and accumulation–area ratio (AAR) methods of calculating glacier equilibrium-line altitudes. *J. Glaciol.* **68** (268), 357–368 (2022).
22. Tadono, T. et al. Precise global DEM generation by ALOS PRISM. ISPRS Annals of the Photogrammetry, Remote Sensing and Spatial Information Sciences, **2**, 71–76. (2014).
23. JAXA. ALOS Global Digital Surface Model ALOS World 3D – 30m (AW3D30) (2025). https://www.eorc.jaxa.jp/ALOS/en/dataset/aw3d30/aw3d30_e.htm. Last accessed Jun 2026.
24. Paul, F., Kääb, A., Maisch, M., Kellenberger, T. & Haeberli, W. Rapid disintegration of Alpine glaciers observed with satellite data. *Geophys. Res. Lett.*, **31**(21). (2004).
25. Larocca, L. J. et al. Glacier equilibrium-line altitude change across Alaska and adjacent Canada indicates a cold, dry Little Ice Age and weaker Aleutian low. *Geophys. Res. Lett.* **53** (4), 2025GL119840 (2026).
26. Bevington, A. R. & Menounos, B. Glaciers in western North America experience exceptional transient snowline rise over satellite era. *Environ. Res. Lett.* **20** (5), 054044 (2025).
27. Zeller, L., McGrath, D., Sass, L., Florentine, C. & Downs, J. Equilibrium line altitudes, accumulation areas and the vulnerability of glaciers in Alaska. *J. Glaciol.* **71**, e28 (2025).
28. Arendt, A. A., Echelmeyer, K. A., Harrison, W. D., Lingle, C. S. & Valentine, V. B. Rapid wastage of Alaska glaciers and their contribution to rising sea level. *Science* **297** (5580), 382–386 (2002).
29. Luthcke, S. B., Arendt, A. A., Rowlands, D. D., McCarthy, J. J. & Larsen, C. F. Recent glacier mass changes in the Gulf of Alaska region from GRACE mascon solutions. *J. Glaciol.* **54** (188), 767–777 (2008).
30. Zemp, M. et al. Global glacier mass changes and their contributions to sea-level rise from 1961 to 2016. *Nature* **568** (7752), 382–386 (2019).
31. Henz, A. et al. Alps-wide high-resolution 3D modelling reconstruction of glacier geometry and climatic conditions for the Little Ice Age. *Cryosphere* **19** (11), 5913–5937 (2025).
32. Larsen, C. F., Motyka, R. J., Freymueller, J. T., Echelmeyer, K. A. & Ivins, E. R. Rapid viscoelastic uplift in southeast Alaska caused by post-Little Ice Age glacial retreat. *Earth Planet. Sci. Lett.* **237** (3–4), 548–560 (2005).
33. Larsen, C. F., Motyka, R. J., Arendt, A. A., Echelmeyer, K. A. & Geissler, P. E. Glacier changes in southeast Alaska and northwest British Columbia and contribution to sea level rise. *J. Geophys. Res. Earth Surf.* **112** (F1), 2004 (2007). (2004).
34. Reinthaler, J. & Paul, F. Assessment of methods for reconstructing Little Ice Age glacier surfaces on the examples of Novaya Zemlya and the Swiss Alps. *Geomorphology.* **461**, 109321 (2004).
35. Reinthaler, J. & Paul, F. Reconstructed glacier area and volume changes in the European Alps since the Little Ice Age. *Cryosphere* **19** (2), 753–767 (2025).
36. Larocca, L. J. et al. Arctic glacier snowline altitudes rise 150 m over the last 4 decades. *Cryosphere* **18** (8), 3591–3611 (2024).
37. MacFee, M., Carrivick, J. L. & Quincey, D. J. Rising snowline altitudes across Southern Hemisphere glaciers from 2000 to 2023. *Sci. Rep.* **15** (1), 35683 (2025).
38. Post, A. S., O'Neel, S., Motyka, R. J. & Streveler, G. P. A complex relationship between calving glaciers and climate. *Eos* **92**, 305–306 (2011).
39. Amundson, J. M. A mass-flux perspective of the tidewater glacier cycle. *J. Glaciol.* **62**, 1–12 (2016).
40. Truffer, M. & Motyka, R. J. Where glaciers meet water: Subaqueous melt and its relevance to glaciers in various settings. *Rev. Geophys.* **54** (1), 220–239 (2016).
41. Frank, T., Åkesson, H., De Fleurian, B., Morlighem, M. & Nisancioglu, K. H. Geometric controls of tidewater glacier dynamics. *Cryosphere* **16** (2), 581–601 (2022).
42. Brinkerhoff, D. J. et al. The demise of the world's largest piedmont glacier: a probabilistic forecast. *Cryosphere* **19** (6), 2321–2353 (2025).
43. McNabb, R. W., Hock, R. & Huss, M. Variations in Alaska tidewater glacier frontal ablation, 1985–2013. *J. Geophys. Research: Earth Surf.* **120** (1), 120–136 (2015).
44. Caldwell, N. G. et al. Retreat and frontal ablation rates for Alaska's lake-terminating glaciers: Investigating potential physical controls with implications for future stability. *J. Glaciol.* **71**, e67 (2025).
45. Otto, D. R., Roe, G. H. & Christian, J. E. An assessment of the disequilibrium of Alaska glaciers. *Cryosphere* **19** (10), 4969–4987 (2025).
46. Carrivick, J. L., Andreassen, L. M., Nesje, A. & Yde, J. C. A reconstruction of Jostedalsbreen during the Little Ice Age and geometric changes to outlet glaciers since then. *Q. Sci. Rev.* **284**, 107501 (2022).
47. Martín-Moreno, R., Allende Alvarez, F. & Hagen, J. O. Little Ice Age' glacier extent and subsequent retreat in Svalbard archipelago. *Holocene* **27** (9), 1379–1390 (2017).
48. Baumann, S., Winkler, S. & Andreassen, L. M. Mapping glaciers in Jotunheimen, South-Norway, during the Little Ice Age maximum. *Cryosphere* **3** (2), 231–243 (2009).
49. Bahr, D. B., Pfeffer, W. T., Sassolas, C. & Meier, M. F. Response time of glaciers as a function of size and mass balance: 1. Theory. *J. Geophys. Research: Solid Earth*. **103** (B5), 9777–9782 (1998).
50. Davies, B. J. & Glasser, N. F. Accelerating shrinkage of Patagonian glaciers from the Little Ice Age (~ AD 1870) to 2011. *J. Glaciol.* **58** (212), 1063–1084 (2012).
51. Grimes, M., Carrivick, J. L., Smith, M. W. & Comber, A. J. Land cover changes across Greenland dominated by a doubling of vegetation in three decades. *Sci. Rep.* **14** (1), 3120 (2024).
52. Von Schuckmann, K. et al. Heat stored in the Earth system 1960–2020: where does the energy go? *Earth Syst. Sci. Data*. **15** (4), 1675–1709 (2023).
53. Carrivick, J. L., Heckmann, T., Turner, A. & Fischer, M. *An assessment of landform composition and functioning with the first proglacial systems dataset of the central European Alps.* 321, 117–128 (Geomorphology, 2018).
54. Carrivick, J., Heckmann, T., Fischer, M. & Davies, B. An inventory of proglacial systems in Austria, Switzerland and across Patagonia. In Geomorphology of proglacial systems: Landform and sediment dynamics in recently deglaciated alpine landscapes (43–57). Cham: Springer International Publishing. (2018).
55. Kavan, J. et al. New coasts emerging from the retreat of Northern Hemisphere marine-terminating glaciers in the twenty-first century. *Nat. Clim. Change*. **15** (5), 528–537 (2025).
56. Ballantyne, C. K. A general model of paraglacial landscape response. *Holocene* **12** (3), 371–376 (2002).
57. Carrivick, J. L. & Heckmann, T. *Short-term geomorphological evolution of proglacial systems.* 287, 3–28 (Geomorphology, 2017).
58. Rick, B., McGrath, D., Armstrong, W. & McCoy, S. W. Dam type and lake location characterize ice-marginal lake area change in Alaska and NW Canada between 1984 and 2019. *Cryosphere* **16** (1), 297–314 (2022).

59. Carrivick, J. L. & Tweed, F. S. Deglaciation controls on sediment yield: Towards capturing spatio-temporal variability. *Earth Sci. Rev.* **221**, 103809 (2021).
60. Carrivick, J. L., Brown, L. E., Hannah, D. M. & Turner, A. G. Numerical modelling of spatio-temporal thermal heterogeneity in a complex river system. *J. Hydrol.* **414**, 491–502 (2012).
61. Fell, S. C., Carrivick, J. L. & Brown, L. E. The multitrophic effects of climate change and glacier retreat in mountain rivers. *BioScience* **67** (10), 897–911 (2017).
62. Bosson, J. B. et al. Future emergence of new ecosystems caused by glacial retreat. *Nature* **620** (7974), 562–569 (2023).
63. Wilkes, M. A. et al. Glacier retreat reorganizes river habitats leaving refugia for Alpine invertebrate biodiversity poorly protected. *Nat. Ecol. Evol.* **7** (6), 841–851 (2023).
64. Rick, B., McGrath, D., McCoy, S. W. & Armstrong, W. H. Unchanged frequency and decreasing magnitude of outbursts from ice-dammed lakes in Alaska. *Nat. Commun.* **14** (1), 6138 (2023).
65. Walden, J. et al. Landslide activation during deglaciation in a fjord-dominated landscape: observations from southern Alaska (1984–2022). *Nat. Hazards Earth Syst. Sci.* **25** (6), 2045–2073 (2025).
66. Coe, J. A., Bessette-Kirton, E. K. & Geertsema, M. Increasing rock-avalanche size and mobility in Glacier Bay National Park and Preserve, Alaska detected from 1984 to 2016 Landsat imagery. *Landslides* **15** (3), 393–407 (2018).
67. Shugar, D. H. et al. A 481-meter-high landslide-tsunami in a cruise ship–frequented Alaska fjord. *Science.* eaec3187. (2026).
68. Bosson, J. B., Huss, M. & Osipova, E. Disappearing world heritage glaciers as a keystone of nature conservation in a changing climate. *Earth's Future*. **7** (4), 469–479 (2019).

Acknowledgements

Frank Paul is thanked for his very helpful feedback on a draft of this paper. Three anonymous reviewers are thanked for their careful scrutiny and constructive comments.

Author contributions

JLC conceived and directed the project, led the mapping, conducted the analysis and drafted the figures and the text. RM, BD, JLS, EL, LJL, ES, RB and JM all contributed to the mapping. RM assisted with the data compilation, mapping tidewater glaciers, and quality checks. JH provided results from his model for selected sub-regions. All authors edited and commented on the text to refine the reporting.

Funding

No funding is associated with this work.

Declarations

Competing interests

The authors declare no competing interests.

Additional information

Supplementary Information The online version contains supplementary material available at https://doi.org/10.1038/s41598-026-70307-w.

Correspondence and requests for materials should be addressed to J.L.C.

Reprints and permissions information is available at www.nature.com/reprints.

Publisher's note Springer Nature remains neutral with regard to jurisdictional claims in published maps and institutional affiliations.

Open Access This article is licensed under a Creative Commons Attribution 4.0 International License, which permits use, sharing, adaptation, distribution and reproduction in any medium or format, as long as you give appropriate credit to the original author(s) and the source, provide a link to the Creative Commons licence, and indicate if changes were made. The images or other third party material in this article are included in the article's Creative Commons licence, unless indicated otherwise in a credit line to the material. If material is not included in the article's Creative Commons licence and your intended use is not permitted by statutory regulation or exceeds the permitted use, you will need to obtain permission directly from the copyright holder. To view a copy of this licence, visit http://creativecommons.org/licenses/by/4.0/.

© The Author(s) 2026